

INVERSE PROBLEMS IN GEOMETRIC GRAPHS USING INTERNAL MEASUREMENTS

MICHAEL ROBINSON

ABSTRACT. This article examines the inverse problem for a lossy quantum graph that is internally excited and sensed. In particular, we supply an algorithmic methodology for deducing the topology and geometric structure of the underlying metric graph. Our algorithms rely on narrowband and visibility measurements, and are therefore of considerable value to urban remote sensing applications. In contrast to the traditional methods in quantum graphs, we employ ideas related to algebraic and differential topology directly to our problem. This neatly exposes and separates the impact of the graph topology and geometry.

1. INTRODUCTION

This article opens a new line of inquiry into the structure of waves on metric graphs. In particular, we are interested in algorithms for recovering the metric graph structure from measurements of propagating waves taken at unspecified locations *within* the graph. We recover this structure in two stages: by first recovering the topology, and then the geometry. The algorithms for each stage draw upon a related circle of ideas in algebraic topology; in particular, we use homological tools to extract topology and cohomological tools to extract geometry. To validate the effectiveness of our approach, the algorithms have been implemented in software and tested on simulation data. [14]

1.1. Historical development of the theory. The study of linear second-order differential operators on metric graphs has a long and venerable history, which is discussed nicely in the survey articles [26] [4] [15], which have extensive references. The study of metric graphs with self-adjoint linear operators began with a short paper by Pauling [36] examining the spectral properties of aromatic compounds. This paper was followed by a number of others that refined Pauling's approach (for instance [40], and of which [38] is a brief summary). Because of the physical chemistry focus, a metric graph paired with a self-adjoint second-order linear operator became known as a *quantum graph*. Because the spectrum of a self-adjoint operator is what is measured in quantum mechanics, the study of quantum graphs has been heavily focused on their spectral properties. The first mathematically rigorous treatment of the spectrum of a quantum graph was by Roth in [39], which introduced the use of *trace formulae*. Trace formulae permit the spectrum of a quantum graph to be treated as a single algebraic object.

This work was supported under DARPA/STO HR0011-09-1-0050 and AFOSR FA9550-09-1-0643.

After Roth's initial work, an increasingly sophisticated literature on spectral properties grew up with trace formulae as the primary tool. As the spectral properties themselves are not of direct interest here, we refer the reader to the excellent survey [15] and will call out a few interesting articles to highlight the historical development of the field. Spacing between eigenvalues in regular and equilateral graphs was treated by [20] and [34]. That the eigenvalues of a quantum graph are generically simple was shown by [12], making use of a generalization of the theory of partial differential operators on manifolds. This simplifies some of the treatment of inverse spectral problems. Post [37] examines some general properties of the spectrum of quantum graphs, and relates them to combinatorial Laplacians. Finally, Parzanchevski [35] showed that two different quantum graphs can have the same spectrum.

In addition to being interesting in its own right, Parzanchevski's article [35] also demonstrates the kind of limitations present in recovering the underlying metric graph from its quantum graph spectrum. In other words, the *inverse spectral problem* [8] cannot be solved completely. In line with spectral methods, which concern globally-valid solutions to linear equations on the quantum graphs, both inverse spectral problems and inverse *scattering* problems concern the extraction of metric graph structure from global measurements. The global nature of these inverse problems is physically helpful, since quantum graphs have been used to study very small objects: it is difficult to excite a single atom in a molecule, usually one must settle for imposing global, *external* excitation.

External excitations lead to scattering problems [31], which in the case of quantum phenomena can lead to rather complicated dynamics for particles confined to a graph [24], [23]. In particular, eigenfunctions of the Laplacian on a quantum graph can have widely separated peaks that are irregularly dispersed in the graph. This permits particles to tunnel in an apparently random fashion from one portion of the graph to another, and has therefore been a good model of quantum chaos. The examination of general scattering problems leads to interesting questions strictly outside of the quantum mechanical context. For instance, Flesia *et al.* [11] examined how the excitation of a regular graph with random speeds of propagation along its supports (or does not support) localized excitations. Indeed, they found that in classical wave propagation, the peaks of eigenfunctions tend to be more widely distributed than in the quantum case.

Inverse spectral problems on quantum graphs became popular following the paper of Gutkin and Smilansky [17], which was made somewhat more precise by Kurasov and his collaborators [27], [29]. Briefly, these articles showed how to solve a generic class of inverse spectral problems when the linear operator is the Laplacian. The nongeneric problems clearly must have symmetries, as [5] explains in detail, and indeed Parzanchevski's examples of isospectral graphs are highly symmetric. For other operators, there are partial results, of which [1] and [45] are typical. For compact graphs in which the self-adjoint operator is the Laplacian, the spectrum determines the total length of the graph (sum of all edge lengths), the number of connected components, and the Euler characteristic (and hence the number of loops) [28].

Clearly, the topology of the underlying metric graph plays an important role in both the spectral structure and the solution to inverse problems. That connection is of particular interest in this article, as we show explicitly how algebraic topological

invariants of the graph impact the spectrum. For instance, in [13], an index is computed that detects traveling wave solutions whose orbits are closed but not periodic when the self-adjoint operator on the graph is the Laplacian. (By “closed but not periodic,” we mean traveling wave solutions that return to their initial starting point, but are going in the opposite direction at that starting point.) This index is topological, and depends only on the Euler characteristic of the graph.

1.2. Main contributions of this article. In this article, we look at quantum graphs from a substantially different viewpoint, motivated by applications in remote sensing. In particular, while we are interested in inverse problems (finding the metric graph structure from measurements), we are interested in gathering *local* information only. To fix ideas, consider a dense urban environment, in which wave propagation can only occur in narrow channels (along the roads), and is obstructed by many buildings. Within this environment are placed an unknown number of transmitters and receivers at various locations. Given that the transmitters can be distinguished from one another by the receivers, how much of the geometric and topological structure of the network of propagation channels can be recovered? Since the propagation channels are narrow, it is sensible to assume that wave propagation happens only along the edges of a graph. The vertices of this graph represent junctions between propagation channels in the usual way. Of course, the resulting second-order operator is the wave operator, which leads to a quantum graph formulation of this problem. (This “thin-wire” approximation has been examined asymptotically in [22], [25], [42], and [32].) Unlike the inverse spectral and scattering problems, the measurements are from *internal* locations, rather than at a distance and concern local features of the data. Indeed, the continuity of the eigenfunctions is what will permit us to infer global features from these local measurements.

There are three main reasons why the traditional quantum graph analytic techniques would be impractical in a remote sensing application:

- (1) In order to collect enough spectral data to exploit any of the inverse problem solutions found thus far, extremely wide-band receivers and transmitters would be needed. In the case of urban remote sensing, the resulting frequencies are usually not available for imaging purposes.
- (2) Propagation losses can be substantial in remote sensing, which usually results in a strong localization of the signal to the vicinity of each transmitter.
- (3) The computational complexity of the algorithms resulting from the inverse spectral problems is unknown, and may hamper practical application.

These difficulties suggest that a better approach is to exploit transmitter visibility information (ie. tabulate which transmitters are visible by which receivers). As will be shown, this permits the topology of the underlying graph to be computed algorithmically and efficiently. We exhibit a novel algorithm for preprocessing visibility information so that it is suitable for computing the underlying topology. Coherent, local measurements of the waves permit the geometry to be recovered, under similar genericity conditions to [17]. Additionally, we obtain a new characterization theorem that relates the space of eigenfunctions to the geometric and topological structure of the graph.

The tools we employ are those in the emerging field of applied algebraic topology. In particular, we will employ the Nerve Lemma [6] to determine the topology from

visibility information, the Whitney embedding theorem for stratified spaces [33], and some ideas from the cohomology of constructible sheaves.

It should be noted that the most similar approach that we have found in the literature is that of the recent work by Caudrelier and Ragoucy [9], which uses reflection-transmission algebras to perform computations on internally-sampled signals. We recover their results using a sheaf-theoretic framework, which cements the connection of their method to topological invariants.

1.3. Outline of the article. We begin in Section 2 by giving a precise statement of the problem we aim to solve, as well as stating the key results that we prove in later sections. In particular, we observe that there exists (Theorem 3) a finite cover by regions coming from thresholded signal levels. This is an enabling result for an algorithm (Algorithm 9) for extracting the graph topology from measurements. We explain this algorithm in Section 3. In Section 4, we demonstrate that once the topology has been found, narrowband signals suffice to compute the geometry (Theorem 36, which has an inductive, algorithmic proof). In support of this result, we prove a characterization (Theorem 23) that shows how the space of solutions to quantum graphs is completely, and explicitly determined by the geometry and topology of the graph. Finally in Section 5 we discuss the results.

2. PROBLEM STATEMENT AND DEFINITIONS

2.1. Review of metric graph definitions. The underlying metric graph structure that will be used in this article is essentially the one initially defined in [46] (and later examined in [3], [2]), but to support the examination of scattering problems we relax the compactness hypothesis.

Definition 1. *A metric graph is a metric space X such that each $x \in X$ has a neighborhood U_x isometric to a degree n_x star-shaped set:*

$$\{z \in \mathbb{C} \mid z = te^{2\pi i k n_x} \text{ for some } 0 \leq t < r_x \text{ and some } k \in \mathbb{Z}\}.$$

We can associate a combinatorial structure of edges and vertices (nonuniquely) to a metric graph. Precisely, if $V \subseteq X$ is a discrete subset such that V contains all points of X whose degree is not 2, we call $V(X)$ a set of *vertices*. The set of path-connected components of the complement of V (each of which is isometric to an open interval) is called the set of *edges* $E(X)$. Those elements of $V(X)$ that lie in the topological closure of an edge e are called the *endpoints* of e . (There may be only one endpoint in any given edge.) (We remark that the choice of vertex and edge sets will in general effect the quantum graph structures we obtain, but we choose vertex conditions for which this nonuniqueness is immaterial.)

We assume that it is always possible to find a *finite* set of vertices and edges. We call X in this situation a *finite metric graph*. With this structure, an edge that contains a degree 1 vertex will be called a *closed edge*. An edge whose closure in X is not a circle, has exactly one endpoint, and has infinite length will be called an *open edge*.

Of course, this assumption replaces the compactness assumption in [46] and others.

The primary contribution of [3] was the formulation of a Laplacian operator suitable for finite metric graphs. For a piecewise smooth function $f : X \rightarrow \mathbb{C}$, this

operator is the bounded, signed *measure* given by

$$(1) \quad \Delta f(x) = \frac{d^2 f}{dx^2}(x) + \sum_{x \in X} \sigma_x(f) \delta_x,$$

where $\sigma_x(f)$ is the sum of (outgoing) directional derivatives of f at x .¹ Notice in particular, that the second derivative operator appearing in the first term of (1) is insensitive to the parametrization at x on the interior of an edge. Secondly, the sum of directional derivatives vanishes everywhere except at finitely many points since f is piecewise smooth. Since the Laplacian is a measure, the fact that the second derivatives are not defined at the vertices presents no difficulty.

2.2. Lossy quantum graphs and their fundamental solutions. Since we are interested in narrowband, lossy wave propagation, we will study the fundamental solution to the Helmholtz equation want to examine solutions to

$$(2) \quad \Delta u + k^2 u = \delta_y,$$

where the wavenumber k may be complex (to indicate lossy propagation), and $y \in X$ is the *transmitter location*. We will be interested in solutions that satisfy the “Kirchoff” conditions [26]:

- u is continuous on X and
- at each point $x \in X$, the sum of the derivatives of u , $\sigma_x(u) = 0$.

Definition 2. *The pairing of (2) and the Kirchoff conditions will be called a lossy quantum graph.*

Clearly, along the interior of an edge, one has the general solution to (2) which is the superposition of two traveling waves:

$$(3) \quad u(x) = c_1 e^{ikx} + c_2 e^{-ikx}.$$

The non-unique choice of vertex and edge sets does not play a significant role in the solutions of a lossy quantum graph when Kirchoff conditions are used. Suppose u is the solution to a lossy quantum graph. If we consider another quantum graph structure in which there is an additional vertex within an edge, u will automatically be a solution of this new structure. Likewise, any solution of this new structure will be a solution of the original structure. This latter fact is most easily seen as a consequence of edge collapse (Lemma 30).

A fundamental solution (2) of a quantum graph X can be obtained as a superposition of solutions of the lossy quantum graph on $X - \{y\}$. It can be interpreted as an external source scattering problem for the graph with y removed.

2.3. Thresholding and covers of contractible regions. In a lossy quantum graph, the energy from a signal source tends to be concentrated around its location. From an urban signal propagation perspective, this means that only receivers nearby a given transmitter will be able to decode its transmissions correctly. This suggests that *visibility* within a lossy quantum graph could be useful for determining which receiver locations are near which transmitters. System designers typically use signal level thresholds to determine whether decoding can proceed successfully, so we employ a thresholding approach to construct visibility regions for a given signal source’s location. Precisely, the region where the signal level is above a given

¹Caution: our sign convention differs from [3].

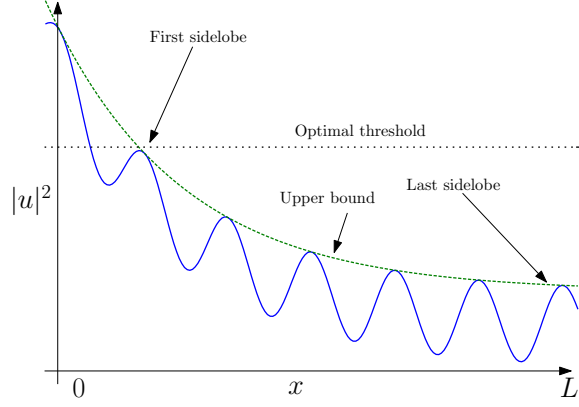


FIGURE 1. Amplitude of interfering traveling waves

threshold will be a contractible subset of X when the threshold and signal loss are large enough.

The central result is that there exists a collection of locations of signal sources that can be thresholded appropriately to give a collection of contractible visibility regions that cover the graph.

Theorem 3. *Suppose X is a lossy quantum graph with wavenumber $k = k' + i\alpha$ for $k', \alpha > 0$. (α is the loss coefficient, with larger values corresponding to higher loss.)*

- (1) *For each $y \in X$, there is a choice of α (say α_y), and a threshold $T_y > 0$ such that for the fundamental solution u_y to (2), the visibility region $U_y(\alpha_y) = \{x \in X \mid |u_y(x)|^2 > T_y^2\}$ is contractible.*
- (2) *The collection $\{U_y(\alpha_y)\}$ forms a cover of X .*
- (3) *Suppose that all vertices of X are contained in the compact set K . There is therefore a finite subcollection $\{y_1, \dots, y_n\}$ such that $\{U_{y_1}(\alpha_{y_1}), \dots, U_{y_n}(\alpha_{y_n})\}$ covers $X \cap K$. Let $\alpha = \max\{\alpha_{y_1}, \dots, \alpha_{y_n}\}$. Then the resulting collection $\{U_{y_1}(\alpha), \dots, U_{y_n}(\alpha)\}$ covers $X \cap K$ and consists of contractible sets.*

In order to prove Theorem 3, we need to study the interference of two lossy traveling waves on a line segment. The requisite information is captured in the following Lemma.

Lemma 4. *Consider $0 \leq x \leq L$ and two traveling waves $u(x) = e^{ikx} + ce^{-ik(x-L)}$ with $k = k' + i\alpha$ as in the statement of Theorem 3. Suppose that $c = \Gamma e^{-\alpha L}$, where Γ is the reflection coefficient at $x = L$. Note that the amplitude of the right-going wave at $x = L$ is $e^{-\alpha L}$. For any fixed Γ , k' , and L , there exists an $\alpha > 0$ and a $T > 0$ such that $\{x \in [0, L] \mid |u(x)| > T\}$ is connected and contains zero.*

Note that T is strictly positive.

Proof. We proceed by computation...

$$\begin{aligned}
 u &= e^{-\alpha x} e^{ik'x} + ce^{\alpha(x-L)} e^{-ik(x-L)} \\
 &= \left(e^{-\alpha x} \cos k'x + ce^{\alpha(x-L)} \cos k'(x-L) \right) + i \left(e^{-\alpha x} \sin k'x - ce^{\alpha(x-L)} \sin k'(x-L) \right).
 \end{aligned}$$

Thus, after a small amount of manipulation,

$$(4) \quad |u|^2 = e^{-2\alpha x} + c^2 e^{2\alpha(x-L)} + 2ce^{-\alpha L} \cos(2k'x - k'L).$$

Notice in particular that the fast spatial variation is captured by the cosine term. The location of the “first sidelobe” (see Figure 1) of this expression is the left most location of the maxima of the cosine, namely

$$x_{FSL} = \frac{n\pi}{2k'} + \frac{L}{2},$$

where n is the smallest integer such that x_{FSL} is positive.

An upper bound for $|u|^2$ is its envelope, namely

$$(5) \quad |u|^2 \leq e^{-2\alpha x} + c^2 e^{2\alpha(x-L)} + 2ce^{-\alpha L}.$$

At the first sidelobe location, the value of $|u|^2$ is

$$\begin{aligned} |u(x_{FSL})|^2 &= e^{-\alpha L} \left(e^{-\frac{\alpha n\pi}{k'}} + c^2 e^{\frac{\alpha n\pi}{k'}} + 2c \right) \\ &= e^{-\alpha L} \left(e^{-\frac{\alpha n\pi}{k'}} + \Gamma^2 e^{\frac{\alpha n\pi}{k'} - \alpha L} + 2\Gamma e^{-\alpha L} \right), \end{aligned}$$

which can be made less than the value at

$$|u(0)|^2 = 1 + \Gamma^2 e^{-3\alpha L} + 2\Gamma e^{-2\alpha L} \cos(-k'L) \approx 1.$$

by taking α large enough. Therefore, we'd like to take $T = |u(x_{FSL})|$.

Now the upper bound (5) is symmetric about $x = \frac{L - \log c}{2}$, so the only thing that could spoil the connectedness of the super-level set of T is large values of $|u|$ near L . Hence, we want

$$\begin{aligned} L &< \text{the last sidelobe location before the minimal envelope} \\ &< L - \log c - \frac{n\pi}{2k'} - \frac{L}{2} \text{ (an underestimate)} \\ \frac{L}{2} &< -\log c - \frac{n\pi}{2k'}. \\ L \left(\frac{1}{2} - \alpha \right) &< -\log \Gamma - \frac{n\pi}{2k'}, \end{aligned}$$

which is clearly satisfied for large enough α . \square

Remark 5. The wavenumber k' is fairly high for practical imaging systems (roughly tens of waves per meter), so one typically spatially averages the measurements to avoid aliasing. This means that instead of thresholding the amplitude (4), we threshold the envelope (5). This results in a tolerance of lower loss, and also results in larger visibility regions.

Now, we can present the proof of Theorem 3:

Proof. (1) This is immediate from repeated application of Lemma 4, and the conversion of each edge incident to a source y into an externally excited edge. The source is at y , and the reflection coefficient Γ captures effects from the rest of the graph as well. Notice that more loss will make Γ smaller, and thus a threshold that satisfies Lemma 4 will continue to work.

(2) That the visibility regions form a cover is immediate from the fact that each region obtained in Lemma 4 contains zero.

- (3) The important point is that for larger α , the sets $U_y(\alpha)$ can be increased in size, or even maintained at the same size (on a single edge) by the selection of a threshold. In any event, it is apparent that since the degree of any vertex is finite, a single threshold per source is easily found that results in cover by contractible sets even when the loss is increased. \square

Remark 6. *Theorem 3 is an existence result only: many configurations of transmitters will fail to provide a cover upon thresholding. However, by adding finitely many more transmitters to areas of low transmitter density, a cover by contractible sets can be obtained.*

3. TOPOLOGY COMPUTATION

In this section, we make use of the visibility regions of the previous section (Theorem 3) to deduce the topology of a quantum graph. Our primary tool is the Nerve Lemma, generally attributed to Leray [6]. If one has a cover of the graph by contractible sets (as in Theorem 3), for which all finite intersections between elements of the cover are also contractible, then one can construct a simplicial space that is homotopy equivalent to the original graph. This *nerve construction* is easy to implement, and for which there are computational topology tools available, for instance [21].

Unlike the work of previous authors, the algorithm presented here (in Section 3.2) only relies on coarse discriminations, rather than on a detailed examination of the spectrum. In particular, the only assessment that is needed is whether the intersection between a number of visibility regions is connected or not. It is not immediately clear that this determination is possible. However, according to a generalization of Whitney's celebrated embedding theorem [30], there is a topology-preserving embedding of the graph into an appropriately high-dimensional signal space, which we construct. The result is that if the intersection of several visibility regions is disconnected, then its image is also disconnected in the signal space.

The main idea of the proof of the algorithm's performance centers around the Mayer-Vietoris sequence for homology, which is a well-understood tool in algebraic topology. We refer the reader to the excellent treatment in [18] for details.

3.1. Uniqueness of signal response and the detection of connected components. If the visibility regions found in Theorem 3 formed a good cover, we would be able to use the Nerve Lemma to recover the homotopy type of the underlying metric graph. However, the visibility regions will usually not form a good cover, often in the way shown in Figure 2. However, in a graph, the intersection of two contractible sets can fail to be contractible only by being disconnected. In this section, we show how to detect disconnectedness of sets by using three or more independent solutions to the quantum graph.

If there are m signal sources, the complete set of measurements we obtain at a receiver located at x is the value of the piecewise smooth function

$$P(x) = (u_1(x), u_2(x), \dots, u_m(x)).$$

For brevity, we say that P is the *signal profile*, taking locations in X to *signal space* S .

If the signal profile is topology-preserving (an embedding), then $U \subseteq X$ is disconnected if and only if its image under P is disconnected. Better, we could just look at the image (which are measurements taken from every point) and deduce the homeomorphism type of the graph. (Indeed, homeomorphism type is stronger than homotopy type.) However, this is unrealistic: normally we have to sample the receiver locations. This is the reason for using a coarser construction based on *refining* the visibility regions into a good cover.

We can obtain the following result (appearing for *manifolds* in [16]) using a stratified transversality result in [44].

Theorem 7. *If the dimension of the signal space m (the number of transmitters) is greater than 2, the signal profile is generically (almost always) an embedding.*

Proof. First, recall that an embedding consists of an injective, piecewise smooth function whose derivative (where defined) is nonvanishing, by the inverse function theorem. By direct computation along the edges, the derivative of a nontrivial solution to the Helmholtz equation is nonvanishing.

It is also therefore the case that a metric graph is an (a)-regular Whitney stratified space. ((a)-regularity is essentially trivial in this case since the only strata are vertices and edges, and vertices have trivial tangent space. See [44] for a precise definition.)

Rather than working with P directly, we work with an augmented version

$$F : C^2(X) \rightarrow C^2(X) \times S \times S,$$

given by

$$F(x, y) = (x, y, P(x), P(y)),$$

where $C^2(X) = X \times X - \Delta_X$ is the space of all *nonoverlapping* pairs of points on the graph. (Δ_X is the diagonal in X and consists of pairs of points at the same location.) We note that C^2 is an (a)-regular stratified space, being the product of two such spaces (removing the diagonal causes no difficulty). Since F is evidently an injective immersion, the image of F is also (a)-regular. (We note that without the factor of C^2 in the codomain, F fails to be injective whenever P is not injective; this disrupts the stratification of the image.)

P fails to be injective if and only if the image of F intersects $D = C^2 \times \Delta_S$. We use transversality to determine whether that intersection is empty or not. The transversality result of [44] states that F is generically transverse to D . (We actually perturb the submanifold D , not the image of F . This amounts to perturbing not the received signals, but our ability to determine if the signals from two points agree. We are looking for an empty intersection between the stratified set and the diagonal. What we get then is stability of this empty intersection.)

When F is transverse to D , then the intersection between any stratum of the image of F and D has dimension no greater than

$$\begin{aligned} \dim C^2 + \dim D - \dim (C^2 \times S \times S) &= 2\dim X + (2\dim X + m) - (2\dim X + 2m) \\ &= 2\dim X - m = 2 - m. \end{aligned}$$

When this bound on dimension is negative, there is no intersection under generic perturbations. Hence, if the number of independent signals measured is greater than 2, the signal profile is generically injective, hence generically an embedding. \square

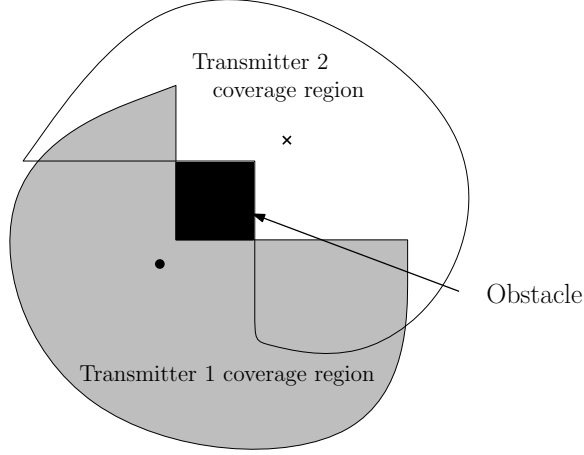


FIGURE 2. Intersection of two contractible coverage regions may be disconnected. (According to Theorem 7, another transmitter would be needed to disambiguate the components of the intersection.)

3.2. Coverage refinement. The visibility regions associated to each transmitter can be made contractible by appropriate thresholding. However, this usually is not enough to make the resulting cover into a “good” cover, and thereby recover the topology. In a graph, the only obstruction is that intersections between coverage regions may be disconnected. In Section 3.1, we showed that disconnected components could be detected and identified from the received signals. In this section we exhibit an algorithm that exploits connected component discrimination to *refine* the coverage regions into a good cover.

In this section, we use homology with a fixed field \mathbb{F} as the set of coefficients. We will therefore suppress the coefficients from the notation. This has the advantage that in graphs, we can identify acyclic sets with contractible ones [21].

Theorem 8. *Suppose that $\mathcal{U} = \{U_1, U_2, \dots, U_n\}$ are open sets forming a good cover of a subgraph of X and that W is a contractible subset of X for which*

- $W \not\subseteq \bigcup \mathcal{U}$, and
- *there are $U_{i_1}, U_{i_2}, \dots \in \mathcal{U}$ such that $W \cap U_{i_1} \cap U_{i_2} \cap \dots$ is disconnected.*

Let $V = W \cap (\bigcup \mathcal{U})$, then

- (1) *each path component of V is acyclic, and*
- (2) *there exist open neighborhoods U'_i of $U_i - V$ for each $U_i \in \mathcal{U}$ and an open neighborhood W' of $W - V$ that satisfy*
 - (a) *$\bigcup \{U'_i\}$ and W' are disjoint open sets,*
 - (b) *each U'_i and W' consists of acyclic path components, and*
 - (c) *the collection of the path components of V , W' , and the U'_i forms a good cover.*

It is straightforward to make use of Theorem 8 to devise an iterative algorithm for refining a set of contractible transmitter coverage regions $\mathcal{V} = \{V_1, V_2, \dots, V_n\}$. We have implemented this algorithm in software and tested it against computer simulations. [14]

Algorithm 9. We define good covers $\mathcal{V}_1, \mathcal{V}_2, \dots, \mathcal{V}_n$ inductively:

- *Base step:* $\mathcal{V}_1 = \{V_1\}$ is a good cover by assumption.
- *Induction step:* Assuming \mathcal{V}_k is a good cover, we apply Theorem 8 with $W = V_{k+1}$ and $\mathcal{U} = \mathcal{V}_k$. We then define \mathcal{V}_{k+1} to be the good cover that we obtain as (2)(c) in Theorem 8.

We begin by proving a technical lemma that we primarily use to relate the homology of a graph to a subgraph. This is an easy application of the Mayer-Vietoris sequence.

Lemma 10. Suppose that $f : X \rightarrow Y$ is a continuous injection from one graph into another and that $Y - f(X)$ is a disjoint union of open, acyclic sets. Then f induces an injection $H_1(X) \rightarrow H_1(Y)$.

Proof. Simplify this proof!! First, observe that there is an open neighborhood U of $f(X)$ that is homotopy equivalent to $f(X)$. This neighborhood consists of the union of $f(X)$ and some subintervals of $Y - f(X)$ (taken from the ends of the edges in $Y - f(X)$ that are adjacent to $f(X)$). Then we may consider the Mayer-Vietoris sequence

$$0 \rightarrow H_1(\text{some intervals}) \rightarrow H_1(U) \oplus H_1(Y - f(X)) \rightarrow H_1(Y) \rightarrow \dots$$

since $U \cup \text{int}(Y - f(X)) = Y$. By assumption U has the same homology as $f(X)$ and X , so this exact sequence can be written

$$0 \rightarrow H_1(\text{some vertices}) \rightarrow H_1(X) \xrightarrow{f_*} H_1(Y) \rightarrow \dots$$

A discrete space always has trivial H_1 , whence f_* must be injective on H_1 . \square

The proof of Lemma 8 relies on the topological dimension of X being not greater than 1. Indeed, the Lemma is false in dimensions 2 and higher.

We now proceed with the proof of Theorem 8.

Proof. Begin by considering the Mayer-Vietoris sequence

$$0 \rightarrow H_1(V) \rightarrow H_1(\cup \mathcal{U}) \oplus H_1(W) \xrightarrow{*} H_1(W \cup (\cup \mathcal{U})) \rightarrow H_0(V) \rightarrow \dots$$

Note that $H_1(W)$ is trivial by assumption, and by Lemma 10 the map $*$ above is injective. Hence each component of V is acyclic, establishing (1).

Define $B_i = U_i \cap (\overline{V} - V) = U_i \cap \partial V$, which consists of the boundary points of V that lie in U_i . Similarly, define $C = W \cap \partial V$.

Observe that C is disjoint from all of the B_i :

$$\begin{aligned} C \cap (\cup B_i) &= (W \cap \partial V) \cap (\cup (U_i \cap \partial V)) \\ &= W \cap (\cup U_i) \cap \partial V \\ &= V \cap \partial V = 0 \end{aligned}$$

since V is open.

Further, ∂V is finite, since X is a metric graph.

Define

$$(6) \quad \delta = \min_{\substack{x, y \in C \cup (\cup \{B_i\}) \\ x \neq y}} d(x, y).$$

Since $C \cup (\cup\{B_i\})$ is finite and contains more than one point, $\delta > 0$. However, an upper bound for δ is

$$(7) \quad \delta < \inf\{d(x, y) | x \in W - V, y \in (\cup\mathcal{U}) - V\}.$$

Define neighborhoods

$$W' = (W - V) \cup \left(\bigcup_{x \in C} B_{\delta/3}(x) \right),$$

and for each i ,

$$U'_i = (U_i - V) \cup \left(\bigcup_{x \in B_i} B_{\delta/3}(x) \right),$$

where $B_r(x)$ is the open ball of radius r centered at x . Evidently by (7), $W' \cap U'_i = \emptyset$ for all i , which establishes (2)(a). By (6),

$$W' \simeq W - V, \text{ and } U'_i \simeq U_i - V.$$

Notice that $H_1(W - V)$ and $H_1(U_i - V)$ are trivial by Lemma 10: consider the inclusion of $W - V \rightarrow W$. We just proved that V is a disjoint union of acyclic components, and it is evidently open. This inclusion induces an injection on H_1 . However, W is acyclic, so this implies that $H_1(W - V)$ must be trivial. The same reasoning works for $U_i - V$, which establishes (2)(b).

To show (2)(c), it remains to establish the following statements, which are immediate from the construction of W' and U'_i :

- Components of V and W' have acyclic intersections since they're precisely half-open intervals,
- Components of V and U'_i have acyclic intersections by the same logic, and
- The collection of components of $\{U'_i\}$ form a good cover of $(\cup\mathcal{U}) - V$. Observe that disjoint intervals were attached to each U_i in the construction of U'_i such that if an interval I_i was attached to U_i and I_j was attached to U_j , with $I_i \cap I_j \neq \emptyset$, then $I_i = I_j$.

□

4. GEOMETRY COMPUTATION

We now address the problem of obtaining the geometric structure of a quantum graph by using a few narrowband measurements taken at points internal to the graph. The central result of this section shows how a single solution over the entire graph determines the geometry up to phase ambiguity. It should be emphasized that this result is obtained under the assumption that the topological structure of the underlying metric graph is known, either as a homeomorphism type (which is preferable), or more likely as a nerve. In either case, we assume that we are in possession of a 1-dimensional simplicial complex that describes the underlying topological space structure of the quantum graph.

Since the primary effect of geometry is on the phase of signals, the measurement of geometric information in a quantum graph requires coherent, time-sensitive processing. From a signal processing perspective, the resulting signal-to-noise requirements are considerably more demanding than those required to obtain visibility information. As a result, the measurements of geometry in a lossy quantum graph will tend to be useful over a fairly small region. We therefore compute geometry

from local measurements, which are the least contaminated by loss. Additionally, we want to operate passively, without reference to known transmitter locations. Therefore, without substantial loss of generality, we consider homogeneous solutions rather than fundamental solutions.

As an aside, the calculations given in this section are actually still valid for *homogeneous* solutions of *lossy* quantum graphs. These solutions correspond to waves incident from outside the graph. (See the discussion following Question 24 for details.)

The space of solutions to a given quantum graph is finite dimensional, and depends on both topology and the geometry. In Section 4.3, we compute this dimension from the graph structure. In more traditional language, we obtain the dimension and structure of the eigenspaces of the graph Laplacian operator. (There is a delicate interplay between loss and the dimension of these eigenspaces: signal loss eliminates resonance phenomena that are extremely useful in inverse spectral methods for detecting geometric and topological features.) *Sheaves* are the appropriate mathematical tool for connecting local information to global behavior, so we develop *sheaf theoretic* computational tools for quantum graphs. We obtain sheaf-theoretic proofs of certain graph operations that preserve quantum graph structure, which allows great computational simplification.

We give a brief introduction to the key ideas of sheaf theory in Section 4.1. For a more detailed exposition, we refer the reader to Appendix 7 of [19] and to [7]. Building on this introductory material, we give an explicit definition of the sheaf structure to be used on a quantum graph in Section 4.2. The global structure of this sheaf is computed in Section 4.3 (Theorem 23), which explicitly demonstrates the topological and geometric dependence of the space of solutions. As an aside, we note how this recovers an inverse spectral result of previous authors. Finally, in Section 4.4, we show how combining the topology and a single solution provides detailed geometric information about the graph.

4.1. A Brief introduction to sheaf theory. A sheaf is a mathematical tool for storing local information over a domain. It assigns some algebraic object, a vector space in our case, to each open set, subject to certain compatibility conditions. These compatibility conditions are of two kinds: (1) those that pertain to restricting the information from a larger to a smaller open set, and (2) those that pertain to assembling information on small open sets into information on larger ones. What is of particular interest is the relationship of the global information, which is valid over the entire graph, to the topology of that graph. Additionally, sheaf theory identifies classes of transformations of the underlying graph that preserve the global information. These transformations permit us to simplify the graphs with no loss of generality.

4.1.1. Elementary definitions for sheaves. In this section, we follow the introduction to sheaves given in Appendix 7 of [19], largely for its direct treatment of sheaves over tame spaces. For more a more general, and more traditional approach, compare our discussion with [7].

Definition 11. A presheaf F is the assignment of a vector space $F(U)$ to each open set U and the assignment of a linear map $\rho_U^V : F(U) \rightarrow F(V)$ for each inclusion $V \subseteq U$. We call the map ρ_U^V the restriction map from U to V . Elements of $F(U)$ are called sections of F defined over U .

Definition 12. A sheaf \mathcal{F} is a presheaf F that satisfies the gluing axioms:

- (Monopresheaf) Suppose that $u \in \mathcal{F}(U)$ and that $\{U_1, U_2, \dots\}$ is an open cover of U . If $\rho_{U_i}^{U_i} u = 0$ for each i , then $u = 0$ in $\mathcal{F}(U)$. Simply: sections that agree everywhere locally also agree globally.
- (Conjunctivity) Suppose $u \in \mathcal{F}(U)$ and $v \in \mathcal{F}(V)$ are sections such that $\rho_U^{U \cap V} u = \rho_V^{U \cap V} v$. Then there exists a $w \in \mathcal{F}(U \cup V)$ such that $\rho_{U \cup V}^U w = u$ and $\rho_{U \cup V}^V w = v$. In other words, sections that agree on the intersection of their domains can be “glued together” into a section that is defined over the union of their domains of definition.

Example 13. Standard examples of sheaves are

- The collection of continuous real-valued functions $C(X, \mathbb{R})$ over a topological space X . In this case, the sections defined over an open set U is $\{f : U \rightarrow \mathbb{R} \mid f \text{ is continuous}\}$.
- The collection of locally constant functions, which essentially assigns a constant to each connected component of each open set.

In contrast, the collection of constant functions does not form a sheaf. Suppose u and v are distinct constants defined over disjoint sets U and V . The sheaf axioms would indicate that since their domains of definition (U and V) are disjoint, then there should exist a constant function defined over $U \cup V$ that restricts to each. This is of course impossible, since such a function is only locally constant.

We now turn to the problem of understanding the effects of graph operations on sheaves. There are six famous operations on sheaves that are important in the general theory, but only two of them (cohomology and direct images) play a role in this article.

4.1.2. Cohomology. We can recast the conjunctivity axiom as testing if $\rho_U^{U \cap V} u - \rho_V^{U \cap V} v$ is zero or not, rather than checking for equality. This can be viewed as looking at kernel of the linear map $d : \mathcal{F}(U) \oplus \mathcal{F}(V) \rightarrow \mathcal{F}(U \cap V)$ given by $d(x, y) = \rho_U^{U \cap V} x - \rho_V^{U \cap V} y$. Indeed, all of the elements of the kernel of such a linear map correspond to the agreement of sections on $U \cap V$.

On the other hand, the monopresheaf axiom indicates that the preimage of zero under the map d corresponds to the restriction of these glued sections onto each of U and V . Indeed, any nonzero element of the *image* of d cannot be a section over $U \cup V$.

These two points motivate a computational framework for working with sheaves, called the Čech construction.

Definition 14. Suppose \mathcal{F} is a sheaf on X , and that $\mathcal{U} = \{U_1, U_2, \dots\}$ is a cover of X . We define the Čech cochain spaces $C^k(\mathcal{U}; \mathcal{F})$ to be the direct sum of the spaces of sections over each k -wise intersection of elements in \mathcal{U} . That is

$$C^k(\mathcal{U}; \mathcal{F}) = \bigoplus \mathcal{F}(U_{i_1} \cap U_{i_2} \cap \dots \cap U_{i_k}).$$

We define a sequence of linear maps

$$d^k : C^k(\mathcal{U}; \mathcal{F}) \rightarrow C^{k+1}(\mathcal{U}; \mathcal{F})$$

by

$$d^k(\alpha)(U_1, U_2, \dots, U_{k+1}) = \sum_{i=0}^{k+1} (-1)^i \rho_{U_0 \cap \dots \cap U_{k+1}}^{U_0 \cap \dots \cap \hat{U}_i \cap \dots \cap U_{k+1}} \alpha(U_0 \cap \dots \cap \hat{U}_i \cap \dots \cap U_{k+1}),$$

where the hat means that an element is omitted from the list. Note that these fit together into a sequence, called the Čech cochain complex:

$$0 \rightarrow C^0(\mathcal{U}; \mathcal{F}) \xrightarrow{d^0} C^1(\mathcal{U}; \mathcal{F}) \xrightarrow{d^1} \dots$$

A standard computation shows that $d_k \circ d_{k-1} = 0$, so that we can define the k -th Čech cohomology space

$$\check{H}^k(\mathcal{U}; \mathcal{F}) = \ker d_k / \text{image } d_{k-1}.$$

The \check{H}^k apparently depend on the choice of cover \mathcal{U} , but for *good* covers (much as in the Nerve Lemma), this dependence vanishes. Leray's theorem for sheaves states that $\check{H}^k(\mathcal{U}; \mathcal{F})$ is the same for each good cover. Indeed, it then depends only on X . So we write $H^k(X; \mathcal{F}) = \check{H}^k(\mathcal{U}; \mathcal{F})$, the sheaf's *cohomology* in the case that \mathcal{U} is a good cover.

A little thought about good covers on graphs reveals two important facts:

- for a metric graph X , $H^k(X; \mathcal{F}) = 0$ for $k > 1$, and
- $H^0(X; \mathcal{F})$ is isomorphic to the space of global sections $\mathcal{F}(X)$.

The first fact follows immediately from a covering dimension argument. The latter fact comes from our construction, and that the image of d^{-1} (*not* d inverse!) is zero. This suggests a computational way to examine solutions to quantum graphs by way of sheaf theory: we construct a sheaf that has local sections being the *locally valid* solutions to the quantum graph, and then compute its cohomology. What is especially valuable about this approach is that there is *additional* information in $H^1(X; \mathcal{F})$. This additional information plays a useful role in Section 4.3 and detects *resonance* phenomena in quantum graphs.

By analogy with the Mayer-Vietoris sequence for homology, there is a Mayer-Vietoris sequence for sheaf cohomology. It is given by the following theorem (also in [7] in a variety of forms):

Theorem 15. *Suppose that A, B are two open subspaces of a graph X that cover X , and that \mathcal{F} is a sheaf over X . Then the following Mayer-Vietoris sequence is an exact sequence:*

$$\dots \rightarrow H^k(X; \mathcal{F}) \xrightarrow{r} H^k(A; \mathcal{F}) \oplus H^k(B; \mathcal{F}) \xrightarrow{d} H^k(A \cap B; \mathcal{F}) \xrightarrow{\delta} H^{k+1}(X; \mathcal{F}) \rightarrow \dots$$

In this sequence, r comes from restriction maps in the obvious way, d is the composition of restriction maps and a difference: $d(x, y) = \rho_A^{A \cap B} x - \rho_B^{A \cap B} y$, and δ is the connecting homomorphism. Note that notation has been abused above slightly: by $H^k(A; \mathcal{F})$ we mean the k -th cohomology of the sheaf \mathcal{F} restricted to subsets lying in A .

4.1.3. Direct images.

Definition 16. *Suppose $f : X \rightarrow Y$ is a continuous function between topological spaces. If \mathcal{F} is a sheaf over X , then the direct image of \mathcal{F} through f is written $f_*\mathcal{F}$ and is given by its action*

$$(f_*\mathcal{F})(U) = \mathcal{F}(f^{-1}(U))$$

on open sets $U \subseteq Y$. Clearly, $f_*\mathcal{F}$ is a sheaf over Y .

The key question is when the cohomologies of \mathcal{F} and $f_*\mathcal{F}$ agree. If they do agree, and the combinatorial structure of Y is much simpler than X , then it is usually much easier to compute the cohomology of $f_*\mathcal{F}$ rather than of \mathcal{F} . We

make extensive use of this in the sequel. This essential question is answered by the following result:

Theorem 17. *(The Vietoris mapping theorem, Theorem 11.1 in Chapter II of [7]) Suppose that $f : X \rightarrow Y$ is a closed, continuous function between metric graphs, and \mathcal{F} is a sheaf over X . If $H^k(f^{-1}(\{y\}); \mathcal{F})$ for $k > 0$ and each $y \in Y$, then \mathcal{F} and $f_*\mathcal{F}$ have isomorphic cohomology.*

4.2. Definition of a sheaf structure for quantum graphs. The collection of locally-valid, continuous solutions to a differential equation on \mathbb{R} forms a sheaf: restricting the domain of validity of a local solution produces a new local solution, and local solutions can be joined if they agree on the intersection of their domains of validity. This construction also works on a quantum graph, resulting in the sheaf of *excitations*.

Since solutions on a single edge consist of two propagating waves, we obtain a more explicit definition for the sheaf of excitations. We construct the sheaf of excitations as a direct image of a sheaf over a directed graph with two oppositely-oriented edges for each undirected edge of our original quantum graph. [26] Our construction permits a slight generalization over the sheaf of excitations in that the values of the solution may take values in any field rather than the complex numbers. This simplifies the notation, so we perform all further computations at this level of generality. The resulting general object is called a *transmission-line sheaf*.

Proposition 18. *Local solutions of a quantum graph form a sheaf, called the excitation sheaf.*

Sheaves provide a convenient way to collate solutions to differential equations. For instance, [43] discusses the situation in great detail for systems of linear partial differential equations. We sketch a proof here for our specific instance.

Proof. The appropriate sheaf is a correspondence between open sets (of the topological space structure of the graph) and the space of continuous functions over them, in which inclusion of open sets corresponds to restriction of functions. Solutions on an open set in the interior of an edge remain solutions when restricted to a smaller domain. Additionally, if solutions on two open sets within the interior of an edge agree (pointwise) on the intersection of these two open sets, then there is a solution defined on the union of these open sets.

The vertex conditions require continuity of solutions and some additional constraints. Suppose that s is a solution defined on U , an open set containing a vertex v . Clearly, s satisfies the vertex conditions at v . Now if $V \subset U$ is another open set, restricting s to V will result in another solution. In particular, if $v \in V$, then the $s|_V$ will still satisfy the vertex condition at v . Now if s_1 and s_2 are solutions defined on U_1 and U_2 , and v lies in $U_1 \cap U_2$, then both s_1 and s_2 will satisfy the vertex conditions at v . If $s_1|(U_1 \cap U_2) = s_2|(U_1 \cap U_2)$, then we can define a new solution s pointwise by

$$s(x) = \begin{cases} s_1(x) & \text{if } x \in U_1 \\ s_2(x) & \text{if } x \in U_2 \end{cases}$$

This new solution clearly satisfies the vertex condition at v , and is otherwise still a solution. \square

The excitation sheaf is a complicated object, one in which the combinatorial structure is obscured. In particular, it is unclear how to compute its sheaf cohomology, which encapsulates all of its associated global structure. Therefore, we construct a new sheaf called a *flow sheaf* with simpler structure that has isomorphic cohomology. The decisive feature of this flow sheaf is that it is *constructible* with respect to the graph structure. This means that over edges or vertices, the sheaf structure is constant. [41] Only where edges attach to vertices does the sheaf structure change, and then only in a constrained fashion.

A flow sheaf, however, is defined over a directed graph. We'll use a direct image construction to write the appropriate sheaf definition for quantum graphs, which are undirected.

Definition 19. *Suppose that \mathbb{F} is a field and that X is a directed graph. Given that X has the usual topology, let $\mathcal{U} = \{U_\alpha, V_\beta\}$ be a base for the topology of X where each U_α is connected and contains exactly one vertex and each V_β is contained in the interior of a single edge. An \mathbb{F} -flow sheaf on X is the sheafification of the following presheaf F , defined on \mathcal{U} :*

- $F(U_\alpha)$ is a direct sum of copies \mathbb{F} , one for each incoming edge into the unique vertex contained in U_α ,
- $F(V_\beta) = \mathbb{F}$,
- if $V_\beta \subset U_\alpha$ and V_β is contained in the n -th incoming edge, the restriction map $F(U_\alpha) \rightarrow F(V_\beta)$ is projection onto the n -th copy of \mathbb{F} ,
- if $V_\beta \subset U_\alpha$ and V_β is contained in the n -th outgoing edge, then there is a fixed \mathbb{F} -linear map $F(U_\alpha) \rightarrow F(V_\beta)$ depending only on the vertex v contained in U_α and n (the outgoing edge). This collection of maps, one for each outgoing edge, is called the local coding at v and is denoted by $\phi_n(v)$.

The following proposition is immediate from the definition of a constructible sheaf.

Proposition 20. *Flow sheaves are constructible with respect to the skeleta of X .*

Now let us consider the more specific case of a direct image of a flow sheaf that is isomorphic to the excitation sheaf defined earlier. Suppose \mathcal{E}_k is an excitation sheaf with wavenumber k over a quantum graph X . Let V and E denote the vertex and edge sets of X , respectively. Denote by L_e the length of edge $e \in E$.

Construct a new graph Y (that is a directed metric graph), by replacing each undirected edge $v_1 \leftrightarrow v_2$ of X by a pair of opposing edges $v_1 \rightarrow v_2$, $v_2 \rightarrow v_1$. Let $f : Y \rightarrow X$ be the map that sends each such pair of directed edges to the corresponding undirected edge of X , as shown in Figure 3. We construct a \mathbb{C} -flow sheaf \mathcal{F} over Y with coding maps tailored to work like the Kirchoff conditions, as follows. Consider a vertex $v \in V$, with degree n in X . Label the incoming edges (in Y) $\{a_1, a_2, \dots, a_n\}$ and the outgoing edges $\{b_1, b_2, \dots, b_n\}$ so that $f(a_i) = f(b_i)$ for each i . Define the coding map by

$$(8) \quad \phi_i(v)(z_1, z_2, \dots, z_n) = \frac{2}{n} \left(\sum_{j=1}^n e^{\sqrt{-1}kL_{a_j}} z_j \right) - e^{\sqrt{-1}kL_{a_i}} z_i,$$

where z_i is the value of a section of \mathcal{F} restricted to the i -th incoming edge

We call $\mathcal{G}_k = f_*\mathcal{F}$ a *transmission line sheaf*. Any sheaf constructed over an undirected graph as the direct image of an \mathbb{F} -flow sheaf with coding maps satisfying

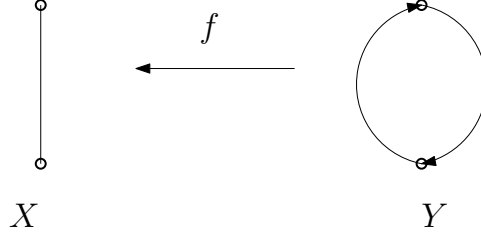


FIGURE 3. Construction of a transmission line sheaf on an undirected graph from a flow sheaf on a directed graph

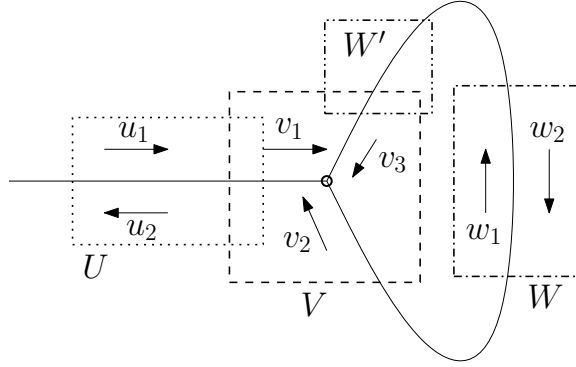


FIGURE 4. Example of a transmission line sheaf

(8) (but with \mathbb{F} endomorphisms specified on the edges, rather than phases) will also be called an \mathbb{F} -transmission line sheaf.

Suppose \mathcal{F} is a transmission line sheaf on a graph X . A *resonant* edge is one in which the edge endomorphisms are identity maps. If the edge endomorphisms differ from the identity, we call the edge *nonresonant*.

Proposition 21. *The excitation sheaf \mathcal{E}_k and the transmission line sheaf \mathcal{G}_k are isomorphic as sheaves. As a result, we may study the solutions to a quantum graph by computing the cohomology of the transmission line sheaf instead.*

Proof. One need only observe that the Kirchoff conditions are equivalent to the coding map (8) employed at the vertices of X , by a straightforward algebraic transformation. \square

Example 22. *Consider the quantum graph shown in Figure 4. This graph has one vertex, one open edge, and one loop edge. Assume that the length of the loop is L . We examine the sheaf on three different open sets, U , V , and W as shown in the figure. The dimension of the space of sections over U and W is 2, and the dimension of the space of sections over V is 3. In the figure, basis elements (in terms of a traveling wave decomposition) are shown.*

If we consider sections that are defined over $U \cup V$, they must agree on $U \cap V$. This induces the following gluing conditions: $u_1 = v_1$ and $u_2 = \frac{1}{3}v_1 + \frac{2}{3}e^{ikL}v_2 + \frac{2}{3}e^{ikL}v_3$.

Observe that since V and W are disjoint, there are no gluing conditions required to construct sections over $V \cup W$. If instead, we moved W to W' , so that $V \cap W' \neq \emptyset$, two gluing conditions apply: $w_1 = v_3$ and $w_2 = \frac{2}{3}v_1 + \frac{2}{3}e^{ikL}v_2 + \frac{1}{3}e^{ikL}v_3$.

4.3. Computation of the space of solutions. The objective of this section is to completely characterize the cohomology of transmission line sheaves in terms of the geometry and topology of the underlying metric graph. The main result is the following theorem:

Theorem 23. *Suppose \mathcal{G} is an \mathbb{F} -transmission line sheaf with on a connected quantum graph that has l closed edges (of which l' of them have edge endomorphisms E that satisfy $E - E^{-1} = 0$, a resonance condition for closed edges), m open edges, and n resonant loops. Then*

$$(9) \quad \dim H^0(X; \mathcal{G}) = \begin{cases} n+1 & \text{if } l = m = 0 \\ n+m & \text{if } l = 0, m \neq 0 \\ n+1 + \min\{0, l' - 1\} & \text{if } l \neq 0, m = 0 \\ n+m + \min\{0, l' - 1\} & \text{otherwise} \end{cases},$$

$$(10) \quad \dim H^1(X; \mathcal{G}) \cong \begin{cases} n+1 & \text{if } l = m = 0 \\ n & \text{if } l = 0, m \neq 0 \\ n+1 + \min\{0, l' - 1\} & \text{if } l \neq 0, m = 0 \\ n + \min\{0, l' - 1\} & \text{otherwise} \end{cases}.$$

This rather long section begins first with a discussion of some of the implications of this result in Section 4.3.1. The proof of Theorem 23 is outlined in Section 4.3.2, with the proofs of the key edge collapse lemmas being postponed until Section 4.3.3.

4.3.1. Sheaf obstruction theory for quantum graphs. Of course, Theorem 23 strongly restricts the geometry of the underlying graph, but it also restricts the topology. In this section, we therefore also answer the question:

Question 24. *Given the cohomology of a transmission line sheaf \mathcal{F} on a quantum graph X , how much does it restrict the topology of X ?*

If there is loss in the quantum graph then no loop and no closed edges are resonant. Therefore, in lossy quantum graphs, the cohomology is entirely determined by the number of open edges and whether there are any closed edges (resonant or not). The space of excitations of a lossy quantum graph is essentially determined by external scattering effects only.

Clearly, a graph with no resonant loops and no resonant edges will have trivial H^1 . The converse is not true, though. Closed edges will typically induce a trivial H^1 if considered on their own, regardless of edge endomorphism. This means that the cohomology of \mathbb{F} -transmission line sheaves is not a strong enough invariant to distinguish between graphs that contain closed edges and those that do not. In particular, consider a graph X that consists of one vertex and n open edges, and a graph Y that consists of one vertex, n open edges, and one closed edge. Regardless of the edge endomorphism for the closed edge in Y , any transmission line sheaf over X will have the same cohomology as any other transmission line sheaf over Y , though clearly their geometry differs. This is a sheaf-theoretic expression of the

existence of isospectral quantum graphs [35], but goes a little farther: there exist isospectral graphs whose eigenspaces agree as well.

A convenient way of summarizing the above discussion is that nontrivial sheaf cohomology classes constitute *obstructions* to the topology of the graph being trivial.

Lemma 25. *Suppose that \mathcal{F} is an \mathbb{F} -transmission line sheaf on a metric graph X which has no closed edges. Then*

- *the number of open edges in X is equal to the Euler characteristic of \mathcal{F} , namely $\chi(\mathcal{F}) = \dim H^0(X; \mathcal{F}) - \dim H^1(X; \mathcal{F})$, and*
- *there are at least $\dim H^1(X; \mathcal{F})$ loops in X .*

The appearance of the Euler characteristic in Lemma 25 fits neatly with the interpretation of H^1 as describing resonances. In particular, one can think of the number of open edges being the total number of excitations ($\dim H^0(X; \mathcal{F})$), which includes both externally-induced excitations and internally-induced excitations (resonances) minus the number of resonances ($\dim H^1(X; \mathcal{F})$). Therefore, the cohomology of the excitation sheaf over a metric graph encompasses both scattering problems and eigenvalue problems.

If we consider the more specific case of lossless excitation sheaves, then the exact number of loops can be determined. Suppose X is a finite metric graph with no closed edges. As noted in Lemma 25, the number of open edges can be computed from the cohomology of any excitation sheaf. Each edge of the graph has a (set of) resonant frequencies, some of which may coincide. Generically, none of the resonant frequencies coincide, and it is therefore easy to locate the lowest resonant frequency of each edge, which determines the length of each edge. This is essentially the idea of [17]. However, the genericity condition can be relaxed, since the cohomology of excitation sheaves captures edge multiplicity information.

This discussion can be summarized by the following proposition and algorithm.

Proposition 26. *The topology and edge lengths of a finite metric graph with no closed edges is completely determined by the cohomologies of the excitation sheaves over it.*

Algorithm 27. *Suppose that X is a finite metric graph with no closed edges, and the \mathcal{E}_k is the excitation sheaf on X with wavenumber k .*

- (1) *Determine the number of open edges m using Lemma 25.*
- (2) *Define*

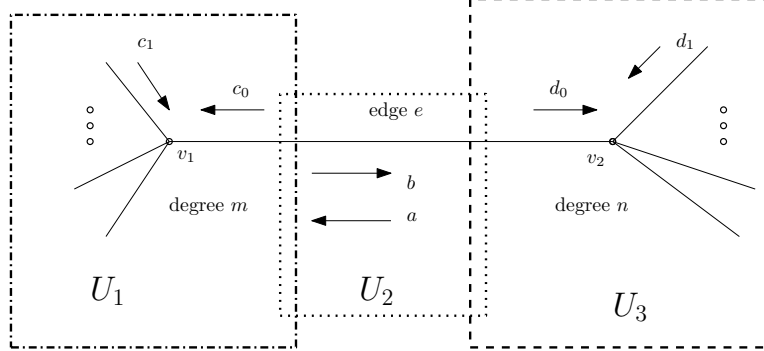
$$S_0 = \begin{cases} \{(k, p) | k \in \mathbb{R}^+ \text{ and } \dim H^1(X; \mathcal{E}_k) = p \neq 0\} & \text{if } m \neq 0 \\ \{(k, p) | k \in \mathbb{R}^+ \text{ and } \dim H^1(X; \mathcal{E}_k) = p - 1 \neq 0\} & \text{if } m = 0 \end{cases}$$

This is the set of resonant wavenumbers of loops in X , counted with multiplicity.

- (3) *Compute $k_i = \min\{k | \text{there exists a } p \in \mathbb{N} \text{ such that } (k, p) \in S_i\}$. This is a fundamental resonant wavenumber of an edge in X . Notice that this is well-defined since S_i is countable.*
- (4) *Define*

$$S_{i+1} = \{(k, p) \in S_i | k \notin k_i \mathbb{N}\} \cup \{(k, p - 1) | (k, p) \in S_i \text{ and } k \in k_i \mathbb{N} \text{ and } p > 1\}$$

- (5) *Iterate steps 3 and 4. Notice that since X is finite, the S_i stabilize at the empty set after finitely many iterations.*


 FIGURE 5. Sets that cover the edge e which is to be collapsed

4.3.2. *Proof of Theorem 23.* The proof relies on three edge collapse results (Lemma 29, Lemma 30, and Lemma 31) that permit combinatorial simplification of the quantum graph without disrupting the structure of the solutions. Combinatorial edge collapse is not new, and plays an important role in the quantum graphs literature, for instance [26]. These lemmas permit a direct, explicit computation of the cohomology of transmission line sheaves. (For a similar computational methodology, which finds a natural incarnation as the sheaf theory we mention here, see [9].)

Definition 28. Suppose that X and Y are finite metric graphs, which may be disconnected. A map $f : X \rightarrow Y$ is called an edge collapse if

- (1) There exists an edge e of X for which $f(e)$ is a vertex of Y ,
- (2) f restricted to $X - e$ is a homeomorphism onto its image, which is $Y - f(e)$.

The first edge collapse lemma applies to a flow sheaf on a directed graph, and is the most general result for these kind of sheaves.

Lemma 29. Suppose that $f : X \rightarrow Y$ is an edge collapse of an edge e that has distinct endpoints, and that \mathcal{F} is an \mathbb{F} -flow sheaf on X . Then f induces an isomorphism on cohomology:

$$(11) \quad H^*(X; \mathcal{F}) \cong H^*(Y; f_*\mathcal{F}),$$

and $f_*\mathcal{F}$ is an \mathbb{F} -flow sheaf on Y in which the coding maps at the vertices in $Y - f(e)$ are unchanged from those in $X - e$. The coding map at e is given by the following. Let v_1 and v_2 be the endpoints of e , in which e is incoming for v_2 . Without loss of generality, suppose that e is the first output of v_1 and the first input to v_2 . Then

$$(12) \quad \phi_i(f(e))(a_1, a_2, \dots, a_m, b_2, b_3, \dots, b_p) = \begin{cases} \phi_{i-1}(v_1)(a_1, a_2, \dots, a_m) & \text{if } i < n - 1 \\ \phi_{i-n}(v_2)(\phi_1(v_1)(a_1, a_2, \dots, a_m), b_2, b_3, \dots, b_p) & \text{otherwise} \end{cases}$$

where the input degree of v_1 is m , the output degree of v_1 is n , and the input degree of v_2 is p . See Figure 5 for a graphical representation of this situation.

It is of course tempting to wonder if multiple edges between a pair of vertices can be collapsed together, something which would be a bit stronger than Lemma 29. The success of this depends delicately on the coding maps. In the case of transmission line sheaves, edge collapse works as desired.

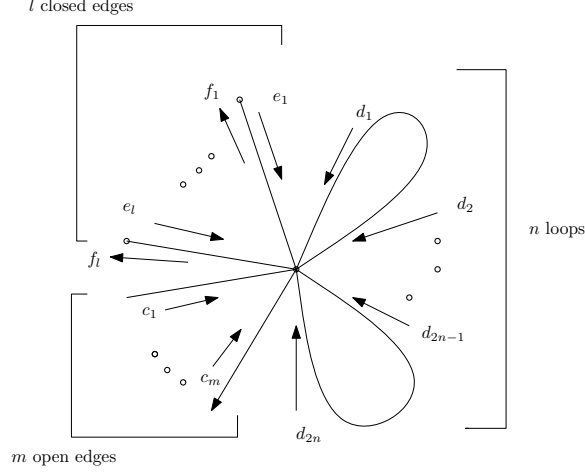


FIGURE 6. A graph with one vertex, l closed edges, m open edges, and n loops

Lemma 30. *Suppose that $f : X \rightarrow Y$ is an edge collapse for an edge e with distinct endpoints, each of which have degree greater than 1. Then for any transmission line sheaf \mathcal{G} with field coefficients, f induces an isomorphism on sheaf cohomology and the direct image $f_*\mathcal{G}$ is also a transmission line sheaf.*

Of course, Lemma 30 specifically excludes the case of collapsing an edge loop, since such an edge does not have distinct endpoints. The final edge collapse lemma permits loops to be collapsed provided they are not resonant.

Lemma 31. *Suppose \mathcal{F} is an \mathbb{F} -transmission line sheaf over a graph X , and $f : X \rightarrow Y$ is a map between graphs that collapses a nonresonant loop. Then f induces an isomorphism on cohomology.*

With these lemmas stated (we prove them in Section 4.3.3), we now address the problem of proving Theorem 23.

Proof. (of Theorem 23) Begin by collapsing out all nonresonant loops using Lemma 31. Then, obtain a minimal spanning tree for X , and collapse each edge in the tree using Lemma 30. Thus the sheaf cohomology of \mathcal{G} can be computed by computing the sheaf cohomology on a graph Y with a single vertex, l closed edges, m open edges, and n loops as shown in Figure 6.

Choose a good cover for this space by selecting U as a contractible open set containing the single vertex of Y . To each loop j , associate two additional open sets K_j, H_j homeomorphic to intervals, which complete the cover as shown in Figure 7.

Note then that the Čech cochain complex is

$$(13) \quad 0 \longrightarrow \mathbb{F}^{m+2n} \oplus \mathbb{F}^{4n} \oplus \mathbb{F}^{2l} \xrightarrow{\delta} \mathbb{F}^{6n} \oplus \mathbb{F}^{2l} \longrightarrow 0.$$

For convenience, let us consider the case where $l = 0$, and let $d = m + 2n$, which is the degree of the single vertex of Y . Organize the coboundary map δ so that it

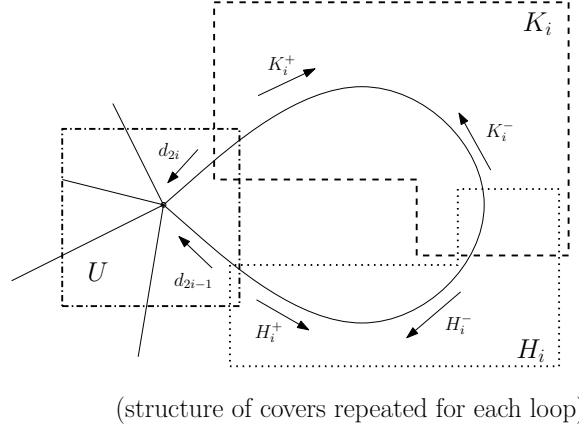


FIGURE 7. Cover over a particular loop in the graph

has the following block form (columns are $c_1, \dots, c_m, d_1, d_2, H_1^+, H_1^-, K_1^+, K_1^-, \dots$):

$$\begin{pmatrix} D_{6 \times m} & B_{6 \times 6} & A_{6 \times 6} & \dots & A_{6 \times 6} \\ D_{6 \times m} & A_{6 \times 6} & B_{6 \times 6} & \dots & A_{6 \times 6} \\ D_{6 \times m} & A_{6 \times 6} & A_{6 \times 6} & \dots & A_{6 \times 6} \\ & & & \dots & \\ D_{6 \times m} & A_{6 \times 6} & A_{6 \times 6} & \dots & B_{6 \times 6} \end{pmatrix}$$

where

$$A_{6 \times 6} = \begin{pmatrix} 0 & 0 & 0 & 0 & 0 & 0 \\ \frac{2}{d} & \frac{2}{d} & 0 & 0 & 0 & 0 \\ \frac{2}{d} & \frac{2}{d} & 0 & 0 & 0 & 0 \\ \frac{2}{d} & \frac{2}{d} & 0 & 0 & 0 & 0 \\ 0 & 0 & 0 & 0 & 0 & 0 \\ 0 & 0 & 0 & 0 & 0 & 0 \\ 0 & 0 & 0 & 0 & 0 & 0 \end{pmatrix},$$

$$B_{6 \times 6} = \begin{pmatrix} 1 & 0 & -1 & 0 & 0 & 0 \\ \frac{2-d}{d} & \frac{2}{d} & 0 & -1 & 0 & 0 \\ \frac{2}{d} & \frac{2-d}{d} & 0 & 0 & -1 & 0 \\ 0 & 1 & 0 & -1 & 0 & 0 \\ 0 & 0 & 1 & 0 & -1 & 0 \\ 0 & 0 & 0 & 1 & 0 & -1 \end{pmatrix},$$

$$D_{6 \times m} = \begin{pmatrix} 0 & 0 & \dots & 0 \\ \frac{2}{d} & \frac{2}{d} & \dots & \frac{2}{d} \\ \frac{2}{d} & \frac{2}{d} & \dots & \frac{2}{d} \\ 0 & 0 & \dots & 0 \\ 0 & 0 & \dots & 0 \\ 0 & 0 & \dots & 0 \end{pmatrix}.$$

We can do row-reduction on each $B_{6 \times 6}$ block individually, and in such a way that this preserves all other entries not in this block (in particular, the nonzero rows

remain unchanged outside the block). We obtain a new block

$$B'_{6 \times 6} = \begin{pmatrix} 1 & 0 & -1 & 0 & 0 & 0 \\ \frac{2-d}{d} & \frac{2-d}{d} & 0 & 0 & 0 & 0 \\ \frac{2-d}{d} & \frac{2-d}{d} & 0 & 0 & 0 & 0 \\ 0 & 1 & 0 & 0 & 0 & -1 \\ 0 & 0 & 1 & 0 & -1 & 0 \\ 0 & 0 & 0 & 1 & 0 & -1 \end{pmatrix},$$

which has rank 4 if $d = 2$ and rank 5 otherwise. Now observe that for the nonzero entries of the second rows of each B' block. They are

$$\begin{array}{cccccc} \frac{2-d}{d} & \frac{2}{d} & \frac{2}{d} & \cdots & \frac{2}{d} \\ \frac{2}{d} & \frac{2-d}{d} & \frac{2}{d} & \cdots & \frac{2}{d} \\ \frac{2}{d} & \frac{2}{d} & \frac{2-d}{d} & \cdots & \frac{2}{d} \\ & & \cdots & & \\ \frac{2}{d} & \frac{2}{d} & \frac{2}{d} & \cdots & \frac{2-d}{d} \end{array}.$$

In each column, there are $n - 1$ copies of $2/d$ and one copy of $\frac{2-d}{d}$, so each column sums to $\frac{2n}{d} - 1$. Now when $n = \frac{d}{2} = \frac{m+2n}{2}$, ie. $m = 0$, this implies that the coboundary matrix has an additional kernel element, and clearly at most one such element. On the other hand, if $n \neq d/2$, clearly all of these second rows of each B' block are linearly independent. Hence

$$\text{rank } \delta = \begin{cases} 4 & \text{if } d = 2 \\ 5n & \text{if } m \neq 0 \\ 5n - 1 & \text{if } m = 0 \end{cases}.$$

Now if $l > 0$, so there are closed edges present, the coboundary map must be augmented with $2l$ rows and columns. Let $d = 2n + m + l$. For the i -th closed edge, we add two new rows, which look like

$$\begin{array}{cccccccccccc} 0 & 0 & \cdots & 1 & -E_i^{-1} & \cdots & 0 & \cdots m \text{ copies} \cdots & 0 & 0 & \cdots 2n \text{ copies} \cdots & 0 \\ \frac{2}{d} & 0 & \cdots & \frac{2-d}{d} & E_i & \cdots & \frac{2}{d} & \cdots m \text{ copies} \cdots & \frac{2}{d} & \frac{2}{d} & \cdots 2n \text{ copies} \cdots & \frac{2}{d} \end{array},$$

in which the first $2l$ columns are added, the next m columns are the first m columns of the original δ , and the remaining columns count off in pairs from the first two columns of each $B_{6 \times 6}$ block. More precisely, they correspond to the columns labelled $e_1, f_1, \dots, e_i, f_i, \dots, e_l, f_l, c_1, \dots, c_m, d_1, \dots, d_{2n}$. After one row operation, this becomes

$$\begin{array}{cccccccccccc} 0 & 0 & \cdots & 1 & -E_i^{-1} & \cdots & 0 & \cdots m \text{ copies} \cdots & 0 & 0 & \cdots 2n \text{ copies} \cdots & 0 \\ \frac{2}{d} & 0 & \cdots & \frac{2}{d} & E_i - E_i^{-1} & \cdots & \frac{2}{d} & \cdots m \text{ copies} \cdots & \frac{2}{d} & \frac{2}{d} & \cdots 2n \text{ copies} \cdots & \frac{2}{d} \end{array}.$$

Note that we thereby obtain a duplicate copy of the second row for each closed edge, so at most 1 is contributed to the rank by these rows. On the other hand, the first row is clearly linearly independent from all the others. Hence the rank of the coboundary map is increased by $\max\{2l, 2l - l' + 1\}$. \square

4.3.3. Proofs of the edge collapse lemmas. We begin by addressing the most general edge collapse result, Lemma 29. The central difficulty is that the edge endomorphisms and coding maps are not specified with a particular form. This complicates the calculations somewhat.

Proof. (of Lemma 29) We aim to employ the Vietoris mapping theorem to obtain the desired isomorphism on cohomology. To this end, observe that since f is an edge collapse, it follows that it is a closed surjection. Additionally, X and Y are both paracompact, so f^{-1} is always taut. Suppose that $y \in Y$, and discern two cases:

- (1) That y is not $f(e)$, in which case f^{-1} is exactly one point, so $H^p(f^{-1}(y); \mathcal{F}) = 0$ for $p > 0$.
- (2) If $y = f(e)$, observe that $H^p(e; \mathcal{F}) = \varinjlim H^p(U_\alpha; \mathcal{F})$, where U_α ranges over open sets containing e . We consider a good cover of U_α that consists of V_1 (containing the vertex v_1) and V_2 (containing v_2) whose intersection lies in the interior of e . The Čech complex is then

$$(14) \quad 0 \longrightarrow M^m \oplus M^p \xrightarrow{\delta} M \longrightarrow 0$$

In which the coboundary map δ is given by $(a_1, a_2, \dots, a_m, b_1, b_2, \dots, b_p) \mapsto \phi_1(v_1)(a_1, a_2, \dots, a_m) - b_1$. Since $\phi_1(v_1)$ is a homomorphism, it's clear that the image of δ is \mathbb{F} . Hence, $H^p(e; \mathcal{F}) = 0$ for $p > 0$.

For the second statement, observe that the only thing to check is that the stalk over $f(e)$ has the correct rank. In this case, that rank is $m + p - 1$, which agrees with Definition 19. \square

Remark 32. *The formula for the coding map at the collapsed vertex $f(e)$ can be written in terms of matrices (with entries in \mathbb{F}). Suppose A is a matrix for $\phi(v_1)$ and B is a matrix for $\phi(v_2)$. Let u^T be the first row of A , which corresponds to the output of v_1 along the edge e . Likewise, let v be the first column of B , which corresponds to the input to v_2 coming from e . Let a and b be the matrices obtained by deleting the first row of A and first column of B , respectively. Then $\phi(f(e))$ has block matrix form*

$$(15) \quad \phi(f(e)) = \begin{pmatrix} a & 0 \\ vu^T & b \end{pmatrix}.$$

Corollary 33. *If \mathcal{F} is an \mathbb{F} -flow sheaf over a finite, connected graph, its sheaf cohomology can be computed by looking at the direct image under the collapse of a spanning tree.*

For the proof of Lemma 30, in addition to verifying that the Vietoris mapping theorem still holds, we must also verify that the direct image is still a transmission line sheaf. This requires a straightforward, but lengthy, computation.

Proof. (of Lemma 30) We need only redo the case of $H^*(f^{-1}(f(e)); \mathcal{F})$ in Lemma 29. In this case, look at a good cover of the edge e , which consists of three sets $\{U_1, U_2, U_3\}$. Let U_1 contain one endpoint of e (degree m), U_3 contain the other (degree n), and U_2 lie entirely within the interior of e . We'll assume that the e has an edge endomorphism L .

In the Čech cochain complex, the coboundary map has the form

$$(16) \quad \begin{pmatrix} 1 & 0 & \dots & 0 & 0 & 0 & \dots & 0 & -L^{-1} & 0 \\ \frac{2-m}{m} & \frac{2}{m} & \dots & \frac{2}{m} & 0 & 0 & \dots & 0 & 0 & -1 \\ 0 & 0 & \dots & 0 & \frac{2-n}{n} & \frac{2}{n} & \dots & \frac{2}{n} & -1 & 0 \\ 0 & 0 & \dots & 0 & 1 & 0 & \dots & 0 & 0 & -L \end{pmatrix},$$

which we claim has rank 2. (The columns are organized by $\mathcal{G}(U_1) \oplus \mathcal{G}(U_3) \oplus \mathcal{G}(U_2)$.) Hence the $H^1(e, \mathcal{G}) = 0$.

We now address the claim by examining the kernel of the coboundary map. By a pair of linear combinations of rows of (16), we obtain

$$d_0 = L \left(\frac{2}{m} \sum_{j=0}^{m-1} c_j - c_0 \right),$$

and

$$c_0 = L^{-1} \left(\frac{2}{n} \sum_{j=0}^{n-1} d_j - d_0 \right).$$

Then we can solve for d_0 by substitution:

$$\begin{aligned} d_0 &= L \left(\frac{2}{m} \sum_{j=1}^{m-1} c_j - \left(\frac{2}{m} - 1 \right) c_0 \right) \\ &= L \frac{2}{m} \sum_{j=1}^{m-1} c_j - \left(\frac{2}{m} - 1 \right) \left(\frac{2}{n} \sum_{j=0}^{n-1} d_j - d_0 \right) \\ &= L \frac{2}{m} \sum_{j=1}^{m-1} c_j - \frac{2}{n} \left(\frac{2}{m} - 1 \right) \sum_{j=1}^{n-1} d_j - \left(\frac{2}{m} - 1 \right) \left(\frac{2}{n} - 1 \right) d_0 \\ \left(1 - \left(\frac{2}{m} - 1 \right) \left(\frac{2}{n} - 1 \right) \right) d_0 &= \frac{2L}{m} \sum_{j=1}^{m-1} c_j + \frac{2}{n} \left(\frac{2-m}{m} \right) \sum_{j=1}^{n-1} d_j \\ \left(\frac{2m+2n-4}{mn} \right) d_0 &= \frac{2L}{m} \sum_{j=1}^{m-1} c_j + \frac{2}{n} \left(\frac{2-m}{m} \right) \sum_{j=1}^{n-1} d_j, \end{aligned}$$

whence

$$(17) \quad d_0 = \frac{nL}{m+n-2} \sum_{j=1}^{m-1} c_j + \frac{2-m}{m+n-2} \sum_{j=1}^{n-1} d_j.$$

In particular, this confirms that the rank of (16) is 2, since the kernel is of dimension $m+n-2$.

Continuing with (17), we show that the direct image is a transmission line sheaf by exhibiting a typical restriction map to an output of one of the edges. Without loss of generality, we consider the output along the i -th edge of v_2 , namely

$$\begin{aligned} d'_i &= \frac{2}{n} \sum_{j=0}^{n-1} d_j - d_i \\ &= \frac{2L}{m+n-2} \sum_{j=1}^{m-1} c_j + \frac{2}{n} \left(\frac{2-m}{m+n-2} \right) \sum_{j=1}^{n-1} d_j + \frac{2}{n} \sum_{j=1}^{n-1} d_j - d_i \\ &= \frac{2}{m+n-2} \left(\sum_{j=1}^{m-1} Lc_j + \sum_{j=1}^{n-1} d_j \right) - d_i, \end{aligned}$$

which is of the form required for a transmission line sheaf. \square

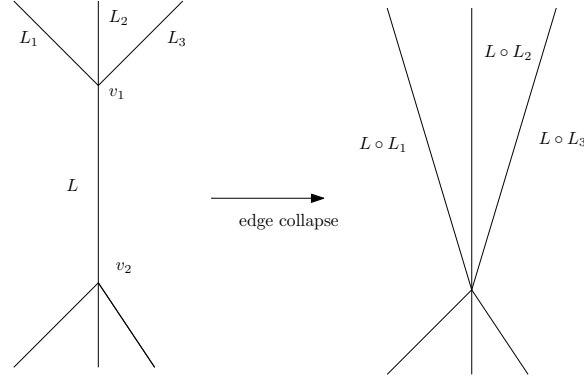


FIGURE 8. Edge collapse results in edge endomorphisms being composed

Remark 34. Notice that when the edge e is collapsed using Lemma 30, the edge endomorphisms on one side are composed (see Figure 8). This composition is non-unique: in the proof, we composed L with the edges on the side of v_1 , but we could have composed by L^{-1} on the side of v_2 . This clearly results in quasi-isomorphic sheaves, as they will agree in cohomology, and this difference will not concern our discussion here.

Remark 35. We note that a degree 1 vertex causes the proof of Lemma 30 to fail because the direct image is generally not a transmission line sheaf. The Vietoris Mapping theorem applies perfectly well in this case, but the coding maps do in fact change. It is true that $H^1(e)$ is still trivial, even if there is a nonidentity edge endomorphism.

Suppose for instance that $m = 1$, and that we wish to compute the restriction to the output of the i -th edge incident to v_2 . This has the value

$$d'_i = \frac{2}{n} \sum_{j=0}^{n-1} d_j - d_i.$$

If it the collapse of the edge resulted in a transmission line sheaf, then we should have

$$d'_i = \frac{2}{n-1} \sum_{j=1}^{n-1} d_j - d_i$$

upon eliminating d_0 using the conditions at v_1 . However, what we instead obtain is

$$d'_i = \frac{2}{n} \left(\frac{L + L^{-1}}{(2/n-1)L + L^{-1}} \right) \sum_{j=1}^{n-1} d_j - d_i,$$

where L is the edge endomorphism for e . Although certain values for L will result in a transmission line sheaf, generic values of L will not.

An interpretation of this result is that the degree 1 vertex's influence is to adjust the coding maps, essentially “tuning” the transmission line. In the case where a transmission line sheaf results from an edge collapse of a closed edge, the edge is the correct length to have no effect at all, which is related to resonance phenomena.

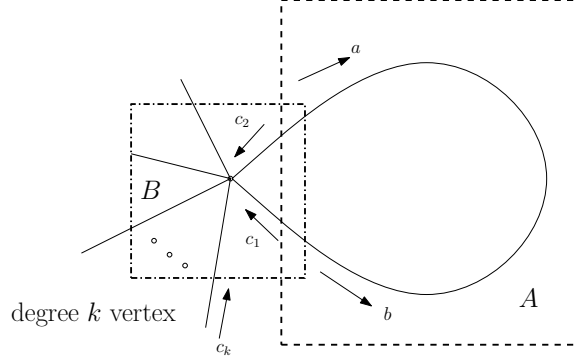


FIGURE 9. Cover of a loop in the graph, for use with the Mayer-Vietoris sequence

Finally, we address the case of Lemma 31. Rather than using the Čech approach as in the earlier calculations, we instead use a Mayer-Vietoris sequence, to illustrate an alternate technique for cohomology computation. This has the advantage of requiring fewer dimensions, and is a fairly natural context to consider the computation of sheaf cohomology over graphs.

Proof. (of Lemma 31) Let U be a connected open set covering the loop to be collapsed, and contain exactly one vertex of degree k . We form a cover of U by two open sets A and B . Let A be a connected open set contained in the interior of the edge, and B be a connected open set containing the unique vertex in U (see Figure 9). Observe that $\mathcal{F}(A) \cong \mathbb{F}^2$ and $\mathcal{F}(B) \cong \mathbb{F}^k$. The appropriate Mayer-Vietoris sequence is

$$0 \rightarrow H^0(U; \mathcal{F}) \rightarrow H^0(A; \mathcal{F}) \oplus H^0(B; \mathcal{F}) \xrightarrow{\Delta} H^0(A \cap B; \mathcal{F}) \xrightarrow{\delta} H^1(U; \mathcal{F}) \rightarrow 0,$$

where we observe that $H^0(A \cap B; \mathcal{F}) \cong \mathbb{F}^4$. As a result of this exact sequence, $H^0(U; \mathcal{F}) \cong \ker \Delta$, and $H^1(U; \mathcal{F}) \cong \text{image } \delta$. Observe that

$$\begin{aligned} \dim \ker \delta &= 4 - (k + 2) + \dim \ker \Delta \\ &= 2 - k + \dim H^0(U; \mathcal{F}). \end{aligned}$$

Suppose that the edge endomorphism for the edge to be collapsed is $L : \mathbb{F} \rightarrow \mathbb{F}$. Then

$$\Delta \left(\begin{pmatrix} a \\ b \end{pmatrix}, \begin{pmatrix} c_1 \\ \vdots \\ c_k \end{pmatrix} \right) = \begin{pmatrix} c_2 - La \\ c_1 - L^{-1}b \\ a - \frac{2}{k}(c_1 + \dots + c_k) + c_1 \\ b - \frac{2}{k}(c_1 + \dots + c_k) + c_2 \end{pmatrix},$$

using Kirchoff conditions at the vertex. Performing some algebraic manipulations, we find that elements of the kernel of Δ satisfy (provided $k \neq 2$)

$$a = - \left(1 - \frac{2}{k}L\right)^{-1} \left(1 - \frac{2}{k}\right) L^{-1}b + \left(1 - \frac{2}{k}L\right)^{-1} \frac{2}{k}(c_3 + \dots + c_k)$$

and

$$0 = \left(1 - \frac{2}{k}L^{-1}\right)b + \left(1 - \frac{2}{k}\right)La - \frac{2}{k}(c_3 + \dots + c_k).$$

If $k \neq 2$, then this leads to

$$0 = (2 - L - L^{-1})b + (L - 1)(c_3 + \dots + c_k),$$

which means that the dimension of the kernel of Δ is $k - 2$ if $L \neq 1$ and $k - 1$ if $L = 1$.

If instead, $k = 2$, then we obtain

$$a = La, \quad b = L^{-1}b,$$

which implies that the dimension of the kernel of Δ is 0 if $L \neq 1$ and 2 otherwise.

Thus we have

$$H^0(U; \mathcal{F}) \cong \begin{cases} \mathbb{F}^{k-1} & \text{if } L = 1 \text{ and } k \neq 2 \\ \mathbb{F}^{k-2} & \text{if } L \neq 1 \text{ and } k \neq 2 \\ \mathbb{F}^2 & \text{if } L = 1 \text{ and } k = 2 \\ 0 & \text{if } L \neq 1 \text{ and } k = 2 \end{cases}$$

and

$$H^1(U; \mathcal{F}) \cong \begin{cases} \mathbb{F} & \text{if } L = 1 \text{ and } k \neq 2 \\ 0 & \text{if } L \neq 1 \text{ and } k \neq 2 \\ \mathbb{F} & \text{if } L = 1 \text{ and } k = 2 \\ 0 & \text{if } L \neq 1 \text{ and } k = 2. \end{cases}$$

The conclusion is that the Vietoris Mapping theorem applies for the loop to be collapsed if and only if it is nonresonant, that is, if $L \neq 1$. \square

4.4. Geometry extraction algorithm. If the topology is known, then generically a single section of the excitation sheaf contains all of the geometric information. This result is stronger than the results obtained by previous authors (like Proposition 26) which requires knowledge of many sections. However, the sheaf-theoretic framework provides a local, iterative mechanism for describing the geometric information in a quantum graph. The central idea is that in collapsing a spanning tree in the graph, the cohomology (and hence the sections) of flow sheaves is unchanged. Under such a collapse, however, the global sections are very easily tied to the metric structure of the graph. By sequentially “undoing” the edge collapses, edge endomorphisms are determined one at a time until all are determined.

Operationally, enough information can be obtained by placing a directional sensor at each vertex with degree not equal to 2. Each such sensor detects the incoming wave amplitude along each incident edge. Since the algorithm measures phase differences between points in the graph, this requires that the sensors be synchronized, and take their measurements simultaneously. From a practical point of view, loss in the graph (which we have neglected in this section) limits the visibility of the signal sources. As such, it is probably unnecessary to require synchronization over all sensors placed in a lossy graph.

Theorem 36. *Suppose that the edge endomorphisms of a transmission line sheaf \mathcal{F} are algebraically independent (in the ring of \mathbb{F} -endomorphisms). In the case of quantum graphs, this is equivalent to requiring that the edge lengths are algebraically*

independent. Then the edge endomorphisms are determined by any nonzero section of \mathcal{F} when Kirchhoff conditions (8) are used.

As might be expected, the proof of this result is more interesting than its statement, and proceeds by an inductive computation.

Proof. Base case: We assume that X consists of a bouquet of circles, namely that there exists a single vertex v in X ; we determine all of the edge automorphisms in \mathcal{F} from s . For concreteness, assume that there are n closed loops and m open edges in X . Consider a connected open set U which contains the unique vertex and none of loops completely. Then $\mathcal{F}(U)$ will be isomorphic to \mathbb{F}^{2n+m} , that is there are $2n+m$ incoming signals entering the vertex. Some of these, of course, will be related if we consider $\mathcal{F}(X)$. Suppose without loss of generality, that $d_1, d_2, \dots, d_{2n-1}, d_{2n}$ are the values of the section s on the loops at v , and that c_1, \dots, c_m are the values of the section s on each open edge at v . We can further organize the loops so that d_j and d_{j+1} are the values at either end of a loop, following Figure 6. Hence, we can use (8) to obtain a set of n equations, one for each loop

$$d_{2j+1} = L_j \left(\frac{2}{2n+m} \left(\sum_{i=1}^m c_i + \sum_{i=1}^{2n} d_i \right) - d_{2j} \right),$$

which can easily be solved for the edge endomorphisms L_j .

Inductive step: We assume that there is a graph Y which can be obtained from X by collapsing $f : X \rightarrow Y$ a single edge e with distinct endpoints v_1, v_2 , and that all edge endomorphisms of $f_*\mathcal{F}$ are known. Assume (see Figure 5):

- That the degree of v_1 is m and that the degree of v_2 is n ,
- That the edge endomorphism of e is L ,
- That c_0, c_1, \dots, c_{m-1} are the values of the section s , that are incoming for v_1 ,
- That c_0 is the value of s coming into v_1 along e , and
- That d_0, d_1, \dots, d_{n-1} are the values of s incoming to v_2 ,

then (8) gives the following equations (see Figure 5 for notation):

$$(18) \quad b = \frac{2}{m}(c_0 + \dots + c_{m-1}) - c_0, \quad a = \frac{2}{n}(d_0 + \dots + d_{n-1}) - d_0.$$

Using the edge endomorphism L , we note that $Lb = d_0$ and $c_0 = L^{-1}a$, which permits each equation in (18) to be solved for d_0 or L .

$$d_0 = \frac{2L}{m}(c_0 + \dots + c_{m-1}) - Lc_0 = \frac{nL}{2-n}c_0 - \frac{2}{2-n}(d_1 + \dots + d_{n-1}).$$

Since the graph X is finite, it only remains to see that the induction can be started by finding a sequence of trees $\emptyset = T_1 \subset T_2 \subset \dots \subset T$ in which $T_i - T_{i-1}$ is a single edge, and T is a spanning tree for X . The base case is obtained by examining $f : X \rightarrow X/T$, and each induction step is obtained by considering the collapse via $f_i : X/T_{i-1} \rightarrow X/T_i$. In each case, these maps satisfy the hypotheses of Lemma 30. \square

5. DISCUSSION

In order to implement our algorithms into a viable sensing system, one needs to address discretization issues. For instance, the topology extraction algorithm assumes that there are enough receivers to discriminate whether a coverage region

(or intersections thereof) is disconnected. This may require a very high density of receivers in order to make this discrimination with confidence, since it essentially amounts to measuring the distance between clusters in signal space. Although such discretization effects are out of the scope of this article, it is useful to note that the amount of loss, the distribution of edge lengths, and the operating frequency play an important role in determining the necessary receiver density.

As a related point, detecting the appropriate threshold to use for the visibility regions is less clear when using discrete receivers. A rigorous approach to this problem might use the tools of persistent homology [10] to attempt to capture the topology of the visibility regions, and select appropriate thresholds.

While the geometry extraction algorithm assumes discrete receivers, their synchronization constitutes a major limitation to performance. Indeed, the synchronization requirement is modulated by the mutual visibility of the receivers, which depends on signal loss. On the other hand, the synchronization requirement may also be relaxed by the use of active sensing, in which the signal sources and sensors are colocated. This method would suggest that instead of studying homogeneous solutions, we instead study fundamental solutions.

Finally, in practical urban imaging applications, the graph model is inaccurate for open areas, though in simulation sensible results can be obtained [14]. Indeed, one needs to generalize the theory discussed here to handle higher-dimensional cellular spaces. Many difficulties arise from this generalization, not the least of which is that the cohomology of the excitation sheaf becomes infinite-dimensional. The refinement algorithm as stated here no longer works correctly, either, as connectedness no longer implies contractibility of intersections. Thresholding to obtain contractibility should still work correctly, though verifying that it does will require considerable effort.

6. ACKNOWLEDGEMENTS

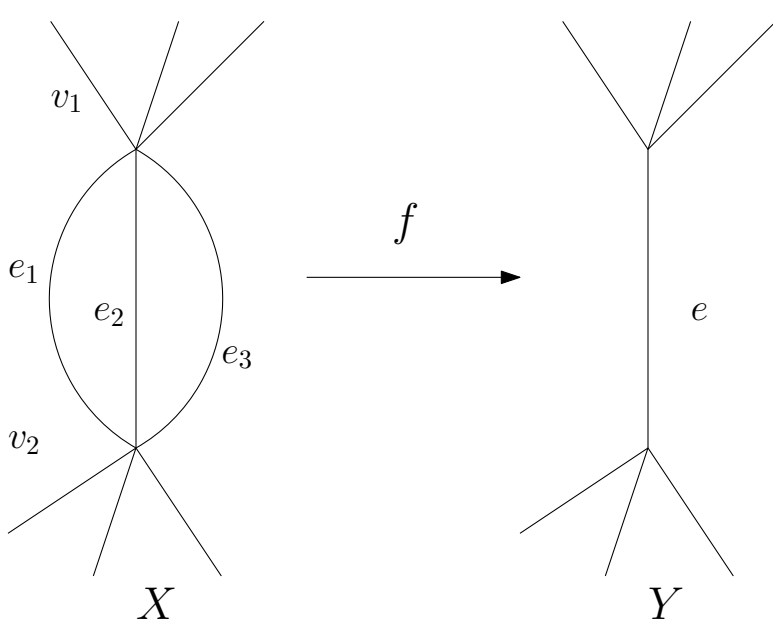
The author wishes to thank Dr. Yuliy Baryshnikov for suggesting the connection of this work to quantum graphs, and Professors Robert Ghrist and Yasu Hiraoka for interesting and valuable discussions on this project. In addition, Hank Owen's "outsider" input helped to refine the exposition.

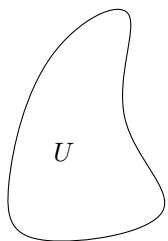
REFERENCES

- [1] Sergei Avdonin and Pavel Kurasov. Inverse problems for quantum trees. *Inverse Problems and Imaging*, 2(1):1–21, 2008.
- [2] Mathhew Baker and Robert Rumely. Harmonic analysis on metrized graphs. *Canad. J. Math.*, 59(2):225–275, 2007.
- [3] Matthew Baker and Xander Faber. Metrized graphs, Laplacian operators, and electrical networks. In *Quantum graphs and their applications*, pages 15–34, 2006.
- [4] Hans-Jürgen Bandelt and Victor Chepoi. Metric graph theory and geometry: a survey. In *Surveys on discrete and computational geometry: twenty years later*, pages 49–87. Amer. Math. Soc., 2008.
- [5] Jan Boman and Pavel Kurasov. Symmetries of quantum graphs and the inverse scattering problem. *Advances in Applied Mathematics*, 35(1):58–70, 2005.
- [6] R. Bott and L. Tu. *Differential forms in Algebraic topology*. Springer, 1995.
- [7] Glen Bredon. *Sheaf theory*. Springer, 1997.
- [8] Robert Carlson. Inverse eigenvalue problems on directed graphs. *Trans. Amer. Math. Soc.*, 351(10):4069–4088, 1999.
- [9] V. Caudrelier and E. Ragoucy. Direct computation of scattering matrices for general quantum graphs. *Nuclear Physics B*, 828(3):515–535, 2010.

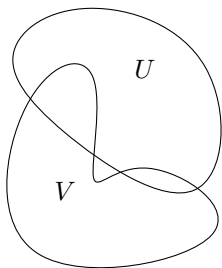
- [10] Herbert Edelsbrunner and John Harer. Persistent homology - a survey. In *Surveys on discrete and computational geometry*, 2008.
- [11] C. Flesia, R. Johnston, and H. Kunz. Strong localization of classical waves: a numerical study. *Europhys. Lett.*, 3(4):497–502, 1987.
- [12] Leonid Friedlander. Genericity of simple eigenvalues for a metric graph. *Israel Journal of Mathematics*, 146:149–156, 2005.
- [13] S. A. Fulling, P. Kuchment, and J. H. Wilson. Index theorems for quantum graphs. *J. Phys. A: Math. Theor.*, 40:14165–14180, 2007.
- [14] R. Ghrist, H. Owen, and M. Robinson. DTIME: discrete topological imaging for multi-path environments. Technical report, University of Pennsylvania (ESE), 2010. Available from <http://repository.upenn.edu/eese-reports/6/>.
- [15] Sven Gnuzmann and Uzy Smilansky. Quantum graphs: Applications to quantum chaos and universal spectral statistics. *Advances in Physics*, 55(5):527–625, 2006.
- [16] Martin Golubitsky and Victor Guillemin. *Stable mappings and their singularities*. Springer, 1973.
- [17] Boris Gutkin and Uzy Smilansky. Can one hear the shape of a graph? *J. Phys. A: Math. Gen.*, 34:6061–6068, 2001.
- [18] Allen Hatcher. *Algebraic Topology*. Cambridge University Press, 2001.
- [19] John H. Hubbard. *Teichmüller Theory, volume 1*. Matrix Editions, 2006.
- [20] Dmitry Jakobson, Stephen Miller, Igor Rivin, and Zeév Rudnick. Eigenvalue spacings for regular graphs, [arxiv:hep-th/0310002v1](https://arxiv.org/abs/hep-th/0310002). 2003.
- [21] Tomasz Kaczyński, Konstantin Michael Mischaikow, and Marian Mrozek. *Computational homology*. Springer, 2004.
- [22] V. Kostrykin and R. Schrader. Kirchoff’s rule for quantum wires. *J. Phys. A: Math. Gen.*, 32:595–630, 1999.
- [23] T Kottos and U Smilansky. Quantum graphs: a simple model for chaotic scattering. *J. Phys. A: Math. Gen.*, 36:3501–3524, 2003.
- [24] Tsampikos Kottos and Uzy Smilansky. Quantum chaos on graphs. *Physical Review Letters*, 79(24):4794–4797, 1997.
- [25] Peter Kuchment. Graph models for waves in thin structures. *Waves in random and complex media*, 12(4):R1–R24, 2002.
- [26] Peter Kuchment. Quantum graphs: an introduction and a brief survey. In *Analysis on Graphs and its applications*, pages 291–312. Isaac Newton Institute for Mathematical Sciences, 2007.
- [27] P Kurasov and F Stenberg. On the inverse scattering problem on branching graphs. *J. Phys. A: Math. Gen.*, 35:101–121, 2002.
- [28] Pavel Kurasov. Graph laplacians and topology. *Ark. Mat.*, 46:95–111, 2008.
- [29] Pavel Kurasov and Marlena Nowaczyk. Inverse spectral problem for quantum graphs. *J. Phys. A: Math. Gen.*, 38:4901–4915, 2005.
- [30] John M. Lee. *Introduction to Smooth Manifolds*. Springer, 2003.
- [31] Hirobumi Mizuno and Iwao Sato. The scattering matrix of a graph. *The Electronic Journal of Combinatorics*, 15(R96), 2008.
- [32] Stanislav Molchanov and Boris Vainberg. Transition from a network of thin fibers to the quantum graph: an explicitly solvable model. In *Quantum graphs and their applications*, pages 227–240, 2006.
- [33] Hiroko Natsume. The realization of abstract stratified sets. *Kodai Math. J.*, 3(1):1–7, 1980.
- [34] Konstantin Pankrashkin. Spectra of Schrödinger operators on equilateral quantum graphs. *Letters in Mathematical Physics*, 77(2):139–154, 2006.
- [35] Ori Parzanchevski and Ram Band. Linear representations and isospectrality with boundary conditions. *J. Geom. Anal.*, 20:439–471, 2010.
- [36] Linus Pauling. The diamagnetic anisotropy of aromatic molecules. *Journal of Chemical Physics*, 4:673–677, 1936.
- [37] Olaf Post. Spectral analysis of metric graphs and related spaces, [arxiv:0712.1507](https://arxiv.org/abs/0712.1507). 2008.
- [38] M. J. Richardson and N. L. Balazs. On the network model of molecules and solids. *Annals of Physics*, 73:308–325, 1972.
- [39] Jean-Pierre Roth. Le spectre du laplacien sur un graphe. In *Colloque de Théorie du Potentiel*, pages 521–539, 1983.
- [40] Klaus Ruedenberg and Charles Scherr. Free-electron network model for conjugated systems: I. theory. *Journal of Chemical Physics*, 21(9):1565–1581, 1953.

- [41] Jörg Shürmann. *Topology and singular spaces and constructible sheaves*. Birkhäuser, 2003.
- [42] Uzy Smilansky and Michael Solomyak. The quantum graph as a limit of a network of physical wires. In *Quantum graphs and their applications*, pages 283–292, 2006.
- [43] D. C. Spencer. Overdetermined systems of linear partial differential equations. *Bull. Amer. Math. Soc.*, 75(2):179–239, March 1969.
- [44] D. J. A. Trotman. Stability of transversality to a stratification implies Whitney (a)-regularity. *Inventiones. Math.*, 50:273–277, 1979.
- [45] V. Yurko. Inverse spectral problems for Sturm-Liouville operators on graphs. *Inverse Problems*, 21:1075–1086, 2005.
- [46] Shouwu Zhang. Admissible pairing on a curve. *Invent. Math.*, 112(1):171–193, 1993.

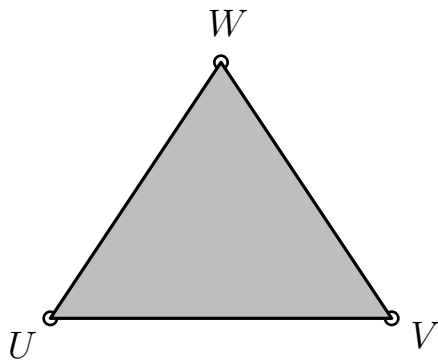
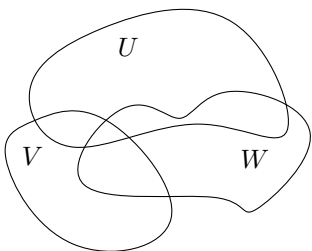




$\circ U$



$U \circ V$



Cover

Nerve